Preparation and photoelectric performance of high-aspect-ratio TiO$_2$ nanotube arrays film electrode

MINGMING DANG[*], YI ZHOU, HONG LI , CAIXIA LV, BIN XIAO, CHANGCHUN GUO, YANCONG OU
College of chemical and biological engineering, Changsha University of Science and Technology, Changsha, 410004, China

TiO$_2$ nanotube arrays film electrodes were fabricated by anodization of Ti foils in an ethylene glycol electrolyte containing 0.25% NH$_4$F and 1V% H$_2$O. The as-prepared nanotubes were characterized by field emission scanning electron microscopy (FESEM), X-ray diffraction (XRD). High-aspect-ratio TiO$_2$ nanotube arrays with tube diameters ranging from 70-100 nm and several micrometers in length were obtained. The samples calcined at 400-500 ℃ showed only anatase phase. The influence of nanotube morphology on the photovoltaic performance of the nanotube arrays film electrodes used in dye sensitized solar cell(DSSC) were investigated by *I-V* characteristics curve. The results indicated that DSSC based on TiO$_2$ nanotube arrays film electrodes fabricated in an ethylene glycol electrolyte containing 0.25% NH$_4$F and 1V% H$_2$O at 45V for 10h exhibited an open circuit voltage of 0.45 V, a short-circuit current density of 4.5 mA/cm^2 and a 0.61 fill factor under simulated AM 1.5 sunlight.

1. Introduction

Dye-sensitized solar cells (DSSCs) based on the photosensitization of a nanocrystalline TiO$_2$ electrode, as designed by Gratzel in 1991, received considerable attention as a potential, cost-effective alternative to silicon solar cells[1]. The certified efficiency of DSSCs based on the nanoparticle TiO$_2$ photoelectrode is 11.2% [2]. This efficiency is still low for commercialization of DSSCs. It was reported that the TiO$_2$ nanoparticle structure has trap sites at the contact region between TiO$_2$ nanoparticles and these could interrupt the transport of electrons in the TiO$_2$ film [3, 4]. Several TiO$_2$ structures such as nanowire [5], nanofiber, nanotube[3, 4, 6], etc., have been applied to DSSCs to overcome the limitation of TiO$_2$ nanoparticle structure. Recently, among these structures, TiO$_2$ nanotube arrays have received a great attention due to their one dimensional structure to provide a direct path for electrons [7]. In application to DSSCs, vertically oriented TiO$_2$ nanotube arrays could potentially improve the charge-collection efficiency by promoting faster transport and slower recombination. So they have higher charge collection efficiencies than a nanoparticle-based structure, as well as better control of the interface makes this morphology desirable for DSSCs [8,9].

TiO$_2$ nanotubes have been prepared by electrochemical anodization[10, 11], hydrothermal synthesis [12,13] and template-assisted synthesis[14]. Electrochemical anodization of Ti metal is a relatively simple approach for systematically altering the morphological properties of nanotube arrays. The anodization potential and fluoride concentration determine the diameter. The length of the nanotubes is tailored by the solution pH and the anodization time. More recently, Frank et al. explored the use of different morphology TiO$_2$ nanotube layers in DSSCs [4]. It was found that for nanotube layers with length of approx 6um a higher effiency could be obtained. To grow longer nanotubes, extended anodization typically in ethylene glycol based fluoride electrolytes is needed.

In this paper, we demonstrate an electrochemical method to prepare TiO$_2$ nanotube arrays by anodization of Ti foils in an ethylene glycol electrolyte containing 0.25% NH$_4$F and 1V% H$_2$O. The high-aspect-ratio TiO$_2$ nanotube arrays could be expected. The morphology and crystal structure of TiO$_2$ nanotube arrays thin film electrodes were characterized. The photovoltaic performance of nanotube film electrodes-based DSSCs were also studied by *I-V* characteristics curve.

2. Experimental details

2.1 Fabrication of nanotube arrays film electrodes

Highly ordered TiO$_2$ nanotube arrays film electrodes were prepared by anodization of Ti foils(99.9%, 0.30mm, Western Metal Materials co., LTD. China) in a two-electrode cell containing a Pt counterelectrode. The anodization was performed at different anodization potential in an ethylene glycol electrolyte containing 0.25% NH$_4$F and 1V% H$_2$O for 10h that resulted in

various nanotube morphology. The as-prepared TiO_2 nanotube samples were rinsed with deionized water and air-dried, then annealed in air for 3h at the temperature of 500 and 600℃ respectively to crystallize the initially amorphous anodized films.

2.2 Fabrication of DSSCs

TiO_2 nanotube arrays film electrodes were dye-sensitized by immersing for 12h in an anhydrous ethanol solution of 0.5 mM N719 dye(cis-bis(isothiocyanato) bis (2,2-bipyridyl 4,4-dicarboxylato) ruthenium(Ⅱ) bis-tet-rabutylammonium) in ethanol. After dye-sensitization, the samples were rinsed with ethanol to remove nonchemisorbed dye. Then the dye-sensitized TiO_2 nanotube arrays film electrodes used as the working electrode and platinum coated fluorine-doped conductive glass as counter electrode to assemble sandwich DSSCs. The electrolyte containing 0.3M lithium iodide(LiI) solution and 0.03M iodide(I_2) solution in acetonitrile were introduced to the gap between the counter and working electrodes by the capillary force.

2.3 Testing and characterization of the samples

The morphology and crystallinity of the TiO_2 nanotube arrays film electrodes were characterized by field emission scanning electron microscopy(FESEM) and X-ray diffraction(XRD). The Current-voltage characteristics were measured with a computer-controlled digital source meter (Keithley, model 2400) under illumination with a Newport solar simulator (AM1.5, 100 mW/cm^2).

3. Results and discussion

3.1 XRD analysis

Fig. 1 (a, b and c) showed XRD patterns of unnealed TiO_2 nanotube arrays and annealed TiO_2 nanotube arrays on Ti foil at 500℃ and 600℃, respectively. As the unnealed TiO_2 nanotube arrays have an amorphous structure, Only Ti peaks were shown in Fig. 1(a). After annealing process at 500℃ for 3h, two broad peaks at $2\theta =$ 25.23^o and 47.88^o which correspond to (101) and (200) plane diffraction of anatase TiO_2 (JPCDS 21-1272) appeared, suggesting that the phase structures of the samples was anatase, which is recommended for the preparation of an optimum dye-sensitized film electrode[15]. However, after annealed at 600℃ for 3h, the intensity of the (101) diffraction peaks of the anatase become weaker, whereas, an additional peak at $2\theta = 27.5$ corresponding to (110) plane diffraction of rutile(IPCDS 87-920) appeared and had stronger peak intensity, indicating that the samples were composed of mixed-phase crystal structure of anatase and rutile.
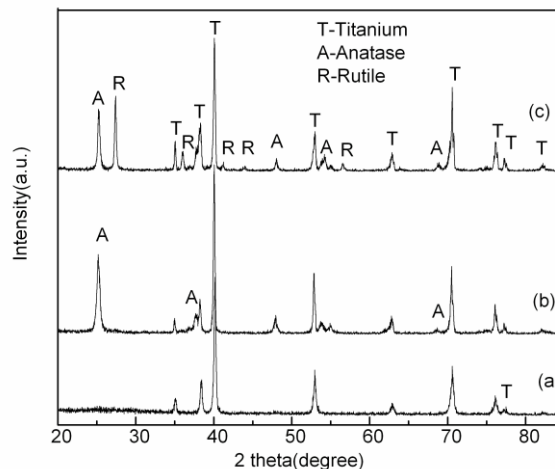

Fig. 1. XRD pattern of TiO₂ nanotube arrays: (a) unannealed TiO₂ nanotube arrays, and annealed TiO₂ nanotube arrays at 500 ℃(b) and 600 ℃(c)

3.2 SEM analysis

Fig. 2 showed the SEM images of TiO_2 nanotube arrays prepared by the electrochemical anodization in an ethylene glycol electrolyte containing 0.25% NH_4F and 1V% H_2O. Anodization is carried out under various applied potentials ranging from 15 to 45 V for 10h. It could be seen from Figure 2a that, the nanoporous structure appeared and some parts of them started to be damaged, the shapes were not very regular on the top. When the anodization potential was 25V(Figure 2b), TiO_2 nanotube arrays could be formed, but the pore diameter was about 70nm and the nanotube length was about 2.9um, respectively. When further increased the potential to 35V(Figure 2c), the TiO_2 nanotube arrays with a regular, well-aligned architecture could be obtained, and the resulting nanotube length increased to 6.5um, and the average diameter was about 85nm. When the anodization potential reached 45V, the nanotube array sample with an average diameter of 100nm have a length of about 8.7um. It could be indicated that the length-to-width aspect ratio of nanotube samples were 41.2, 76.5 and 87.0 as the anodization potential increased from 25V, 35V, and 45V, respectively. This was due to the fact that with anodization potential increasing, the electrochemical etching rate at the bottom of the tubes(field assisted oxidation of Ti and electrical dissolution of TiO_2) and the rate of chemical dissolution also increased, resulting in longer nanotube arrays of greater diameter [16, 17]. For a given the tube diameter, the increased anodization potential enabled substantial increases in the nanotube length, which was attributed to that the larger anodization potential increased driving force for ionic transport through the barter layer at the bottom of the pore resulting in faster movement of the Ti/TiO_2 interface into the Ti metal. Therefore, within

certain range for anodization potential, increasing anodization potential could enhance the length-to-width
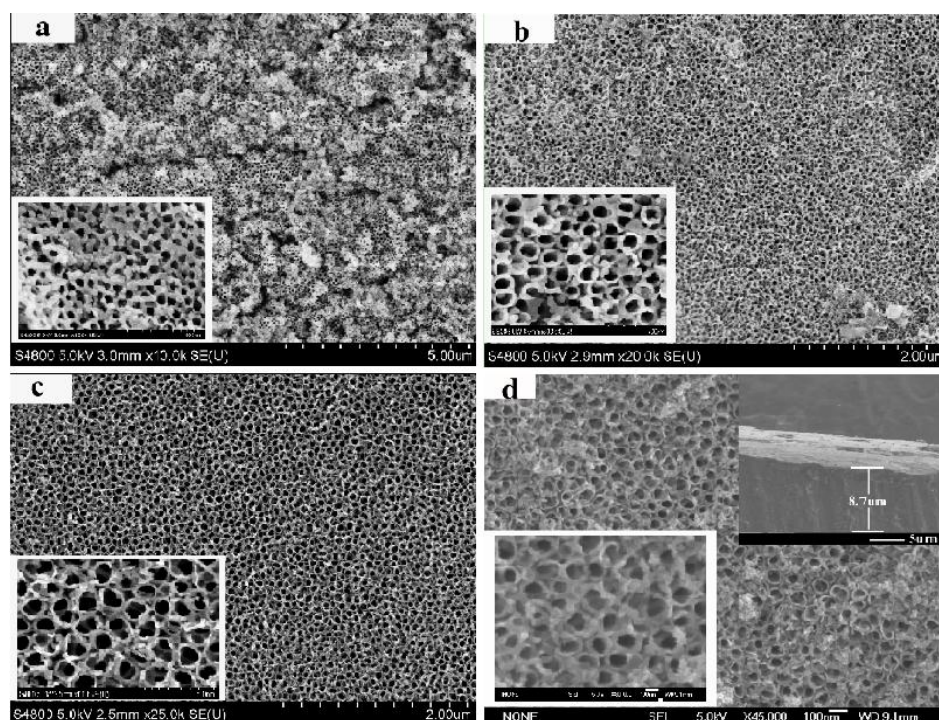
aspect ratio of nanotube arrays.

Fig. 2. SEM images of TiO$_2$ nanotube made with different anodization potential: (a) 15V; (b) 25V; (c) 35V and (d) 45V. The insets are the magnified views of the surfaces

3.3 The formation mechanism of TiO$_2$ nanotube arrays

Fig. 3 showed the current-time behaviour during potentiostatic 10V anodization of a Ti foil sample in an ethylene glycol electrolyte containing 0.25% NH$_4$F and 1V% H$_2$O. The behavior of the current transient in this solusion was similar to the transient observed in aqueous acid fluoride solution. However, It was noteworthy that the anodization process in this solution was slower than that of the aqueous fluoride solution because of a higher viscosity in the ethylene glycol electrolyte containing 0.25% NH$_4$F and 1V% water. It could be seen that the anodization current dropped sharply from a high initial value in the first 100 seconds of anodization due to initial formation of an insulating oxide layer and then a region where the current increased and reached a well-defined plateau because of pitting of the oxide layer by fluoride ions. Thereafter, the anodization current decreased with a slightly shallower slope. Lastly, the anodization current remains relativelt constant after about 1500s. During the initial period, gas evolution at the anode was observable. Since gas evolution required electronic charge transfer, this was indicative of electronic conduction dominating in the early part of the process.
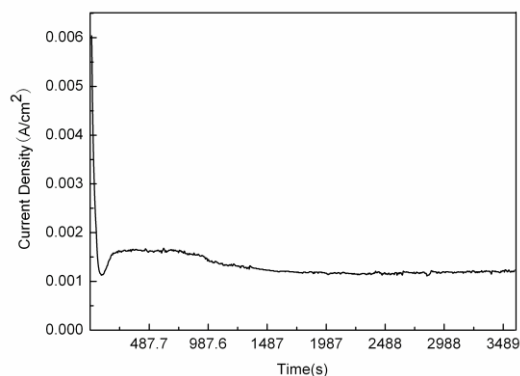

Fig. 3 The current-time behaviour during potentiostatic 10V anodization of a Ti foil sample in an ethylene glycol electrolyte containing 0.25% NH$_4$F and 1V% H$_2$O

3.4 Photoelectric performance of DSSCs based on TiO$_2$ nanotube arrays film electrodes

Fig. 4 showed Current-voltage characteristics of DSSCs based on TiO$_2$ nanotube arrays film electrodes fabricated in an ethylene glycol electrolyte containing 0.25% NH$_4$F and 1V% H$_2$O at different anodization voltage for 10h.
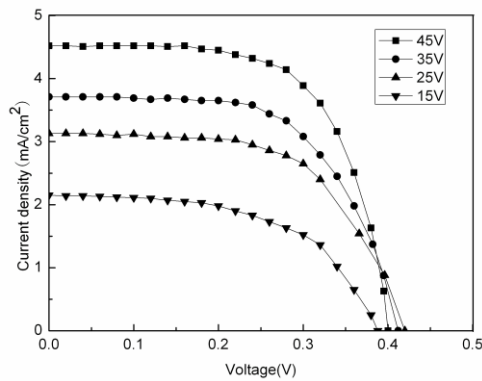
Fig. 4   Current-voltage characteristics of DSSCs based on TiO$_2$ nanotube arrays film electrodes fabricated in an ethylene glycol electrolyte containing 0.25% NH$_4$F and 1V% H$_2$O at 15, 25,35 and 45V for 10h.

Detailed photovoltaic performance parameters of DSSCs for films with different anodization potential were presented in Table 1. It was evident that as the anodization potential increasing, the short circuit current density(Jsc) also increased. This might be due to increasing nanotube in length and the tube diameter with anodization potential increased(as shown in Fig. 2), indicating a higher surface area of the resulting nanotube arrays, which enabled higher surface available for dye chemisorption, resulting in increasing the photoproduction electron. However, The open circuit voltage decreased slightly with increasing anodization potential.

Table 1. Current-voltage characteristics of DSSCs based on TiO$_2$ nanotube arrays film electrodes under simulated AM 1.5 light

Sample	Anodization Voltage(V)	L（um）	Jsc(mA/cm^2)	Voc(V)	FF(%)
1	45	7.8	4.5	0.45	0.61
2	35	6.5	3.7	0.46	0.58
3	25	2.9	3.1	0.48	0.56
4	15	—	2.2	0.44	0.53

This might be attributes to the fact increasing the surface area of nanotube arrays could obtained more injected electrons, which could make the recombination possibility of injected electron on TiO$_2$ nanotube array thin films and electron acceptor ion in the electrolyte increased[18], resulting in the dark current (i_o) inceased. According to the formula:

$$V_{0C} = (\frac{nRT}{F})\ln\left(\frac{i_{sc}}{i_o}-1\right) \qquad (1)$$

Hence, it could be found that the open circuit voltage(Voc) decreased.

4. Conclusions

In conclusion, we investigated the morphology and crystallinity and photovoltaic performance of DSSCs based TiO$_2$ nanotube arrays prepared from electrochemically anodizing Ti foils. High-aspect-ratio TiO$_2$ nanotube arrays with tube diameters ranging from 70-100 nm and and several micrometers in length were

obtained. The pore diameter and the length of the TiO$_2$ nanotubes increased when the anodization potential changed from 15V to 45V. The nanotube arrays were fully crystalline with the anatase under calcined at 500 ℃ for 3h. It was observed that increasing the anodization voltage leaded to increasing the short circuit current density(Jsc) and decreasing slightly the open circuit voltage(Voc) of DSSCs based TiO$_2$ nanotube arrays film electrodes. Finally, varying the electrochemical fabrication conditions was known to affect the geometry and surface properties of the nanotube arrays. Investigations of the consequences of these morphological changes on the photoconversion processes are likely to improve significantly the photovoltaic performance of DSSCs based TiO$_2$ nanotube arrays film electrodes.

References

[1] B. O′ Regan, M. Gratzel, Nature. 737, 353 (1991)

[2] M. A. Green, K. Emery, Y. Hishikawa, W. Warta, Prog. Photovoltaics Res. Appl. **17**, 320 (2009)

[3] G. K. Mor, K.Shankar, M.Paulose, O.K.Varghese, C.A.Grimes, NanoLett. **6**, 215 (2006)

[4] K. Zhu, N. R. Neale, A. Miedaner, A. J. Frank, NanoLett. **7**, 69 (2007)

[5] M. Adachi, Y. Murata, J. Takao, J. Jiu, M. Sakamoto, F. Wang, J. Am. Chem. Soc. **126**, 14943 (2004)

[6] K. Shankar, G. K. Mor, H. E. Prakasam, S. Yoriya, M. Paulose, O. K. Varghese, C. A. Grimes, Nanotechnol. 18, 065707(11pp.) (2007)

[7] J. M. Macak, H. Tsuchiya, P. Schmuki, Angew. Chem. Int. Ed. **44**, 2100 (2005).

[8] M. Gratzel, J. Photochem. Photobiol. A: Chem. **168,** 3 (2004).

[9] M. Adachi, Y. Murata, I. Okada, S. Yoshikawa, J. Electrochem, Soc. **8**(150), 488 (2003).

[10] G. K. Mor, O. K. Varghese, M. Paulose, C.A. Grimes, Adv. Funct. Mate., **8**(15), 1291 (2005).

[11] J. M. Macak, H. Tsuchiya, L. Taveira, S. Aldabergerova, P. Schmuki, Angew. Chem. Int. Ed. **45**(44), 7463 (2005)

[12] T. Kasuga, M. Hiramatsa, A. Hoson, T. Sekino, K. Niihara, Langmuir. **14**, 3136 (1998).

[13] Q. Chen, W. Z. Zhou, G. H. Du, and L. M. Peng, Adv. Mater. **7**(14), 1208 (2002)

[14] M. S. Sander, M. J. Cote, W. Gu, B.M. Kile, C. P. Tripp, Adv. Mater. **22**(16), 2052 (2004)

[15] N. G. Park, J. V. Lagemaat, A. J. Frank, J. Phys. Chem. B. **104**(38), 8989 (2000)

[16] S. Kaneco, Y. S. Cheng, P. Westerhoff, J. C. Crittenden, Scr. Mater. **56**, 373 (2007).

[17] G. K. Mor, O. K. Varghese, M. Paulose, K. Shankar, C. A. Grimes, Sol. Energy Mater. Sol. Cells. **90**, 2011 (2006)

[18] S. Dai, J. Weng, Y. Sui, C. Shi, Y. Huang. S. Xiao, S. Chen, L. Hu, F. Hong, K. Wang, Sol. Energy Mater. Sol. Cells. **84**, 125 (2004)

_____

*Corresponding author: dangmm1985@163.com,